REPORT DOCUMENTATION PAGE

The public reporting burden for this collection of information is estimated to average 1 hour per response, including the time for reviewing instructions, searching existing data sources, gathering and maintaining the data needed, and completing and reviewing the collection of information. Send comments regarding this burden estimate or any other aspect of this collection of information, including suggestions for reducing the burden, to Department of Defense, Washington Headquarters Services, Directorate for Information Operations and Reports (0704-0188), 1215 Jefferson Davis Highway, Suite 1204, Arlington, VA 22202-4302. Respondents should be aware that notwithstanding any other provision of law, no person shall be subject to any penalty for failing to comply with a collection of information if it does not display a currently valid OMB control number.
PLEASE DO NOT RETURN YOUR FORM TO THE ABOVE ADDRESS.

1. REPORT DATE *(DD-MM-YYYY)*	2. REPORT TYPE	3. DATES COVERED *(From - To)*
08/08/2008	Final Report	01/01/2005 - 02/28/2008

4. TITLE AND SUBTITLE

Investigation of new Isotactic Polypropylene and Syndiotactic Polystyrene Materials for High Pulsed Power Capacitors

5a. CONTRACT NUMBER

5b. GRANT NUMBER

N00014-05-1-0287

5c. PROGRAM ELEMENT NUMBER

6. AUTHOR(S)

Chung, Mike
Langston, Justin, A.

5d. PROJECT NUMBER

5e. TASK NUMBER

5f. WORK UNIT NUMBER

7. PERFORMING ORGANIZATION NAME(S) AND ADDRESS(ES)

The Pennsylvania State University
Office of Sponsored Programs
110 Technology Center Building
University Park, PA 16802-7000

8. PERFORMING ORGANIZATION REPORT NUMBER

9. SPONSORING/MONITORING AGENCY NAME(S) AND ADDRESS(ES)

Office of Naval Research
875 North Randolph Street
Arlington, VA 22203-1995

10. SPONSOR/MONITOR'S ACRONYM(S)

ONR

11. SPONSOR/MONITOR'S REPORT NUMBER(S)

12. DISTRIBUTION/AVAILABILITY STATEMENT

Approved for Public Release; distribution is Unlimited

13. SUPPLEMENTARY NOTES

The bi-axially oriented LCBPP films were prepared by the collaboration with Mr. Tom Ramotowski at NUWC (Newport) and Professor Eric Baer at Case Western Reserve University.

14. ABSTRACT

Under this ONR program, we have been studying two new polymers, including long chain branched polypropylene (LCBPP) and PVDF copolymers, toward the Navy capacitor goal with energy density >30 J/cc and low energy loss. The approach in LCBPPs is to increase breakdown strength by preparing high quality thin films via the combination of LCB structure and bi-axially stretching. The experimental results show some high quality LCBPP thin films, exhibiting a very high breakdown electric field >1000 MV/m, energy density ~13 J/cm3 (about 10 times higher than that of the current state-of-the-art PP capacitor), and nearly no energy loss. On the other hand, in the PVDF copolymers containing polar crystals, the research has been focusing on the polarization-depolarization profile. Some VDF/TrFE/CTFE terpolymers with relaxed dielectric properties provide both AC and DC powered capacitors with a relatively balanced property. The optimum one (VDF/TrFE/CTFE = 65.6/26.7/7.7 mol%) shows a charging energy density >20 J/cm3 at E =500 MV/m, but with a significantly high energy loss >30% during the discharging cycle. Overall, a significant progress has been made in the past three years. However, both polymers are far from the Navy capacitor goal (>30 J/cm2 and low loss).

15. SUBJECT TERMS

high energy density capacitor, high pulsed power capacitor, polypropylene, LCBPP, PVDF.

16. SECURITY CLASSIFICATION OF:			17. LIMITATION OF ABSTRACT	18. NUMBER OF PAGES	19a. NAME OF RESPONSIBLE PERSON
a. REPORT	b. ABSTRACT	c. THIS PAGE	SAR		19b. TELEPHONE NUMBER *(Include area code)*

Final Program Report for the ONR Program on

Investigation of new Isotactic Polypropylene and Syndiotactic Polystyrene Materials for High Pulsed Power Capacitors

Principle Investigator: T. C. (Mike) Chung
Contract/Grant Number: N00014-05-1-0287

Summary:

Under this ONR research program, we have been studying long chain branched polypropylene (LCBPP) and PVDF based copolymers for the metalized polymer film capacitors. The objective is to achieve Navy capacitor goal with high energy density (30 J/cc) and low loss. We have developed several synthesis routes to prepare both new polymers and evaluated their capacitor performances. LCBPP polymers were synthesized via a combination of metallocene catalyst, such as rac-Me$_2$Si(2-Me-4-Ph-Ind)ZrCl$_2$/MAO, and a T-reagent (branching agent). On the other hand, the fluoropolymers were prepared by a new borane/oxygen control radical initiator in a homogeneous solution at ambient temperature. Some significant progresses have been reported in 13 published papers, 8 issued patents and patent applications.

We have also developed a method to prepare well-defined LCBPP polymers with pre-determined backbone and branch molecular weights, and branch density before coupling reaction. The systematic examination shows dramatic difference between LCBPP and linear (commercial) PP. Under elongation flow, a LCBPP polymer with 3 branches (molecular weight of backbone: 100k and branches: 30k) exhibits an extensional viscosity 180 times higher than the corresponding linear PP having similar molecular weight. This large strain hardening is very important in film-blowing or foaming processes, by providing crucial melt stability to films and forms. By collaborating with Professor Eric Baer (CWRU) and Tom Ramotowski (NUWC), we have obtained several uniform bi-axially oriented LCBPP thin films (thickness ~5 μm) with good mechanical properties. Some of the films exhibit a very high breakdown electric field >1000 MV/m, with a discharging energy density ~13 J/cm^3 (almost 10 times of the current state-of-the-art PP capacitor) and very low energy loss. On the other hand, the PVDF-based fluoropolymers are very dependent on the composition. Ferroelectric VDF/TrFE copolymers, having all-trans chain conformation and huge remnant polarization, are not suitable for capacitor applications. The poled PVDF homopolymer and VDF/CTFE copolymers show limited potential for DC powered capacitors. Some VDF/TrFE/CTFE terpolymers, with small γ-phase crystals, relaxed dielectric properties (no remnant polarization), and Curie transition at near ambient temperature, provide both AC and DC powered capacitors with a balance of properties—high energy density and relatively low energy loss. The best relaxed ferroelectric VDF/TrFE/CTFE (65.6/26.7/7.7) terpolymer, with high dielectric constant (>60, 1 kHz) at Curie temperature (Tc ~35 ^{o}C), is stable up to 500 MV/m of the applied electric field, displaying similar releasing energy density ~13 J/cm^3, but with significantly large energy loss (>30%).

Overall, LCBPP and PVDF copolymers show completely different polarization-depolarization profiles, with the induced polarization happened in LCBPP and the polar group (crystal) orientation occurring in PVDF copolymers. Although significant progresses have been made, both systems are still far from the ideal case of high energy density and low loss.

20080922206

Objectives:

This R&D program focuses on the development of new polymeric material to address Navy's needs in future high energy capacitors for pulsed power electric guns. The major objective is to achieve high energy density >30 J/cc in material level with low dielectric loss (tanδ <0.01). In addition, the material shall also be stable at elevated temperature, self-healing after a puncture, long term stability under stress, cost effective, easy processing into uniform metalized thin films (thickness <10 µm), and scale-up for commercialization.

Approach:

Since PP exhibiting many desirable properties (low loss, self-healing, low cost, etc.) and the industrially favorable capacitor polymer (with established capacitor fabrication technology), our research strategy has been focusing on the improvement (chemical modification) of PP polymers to address its short-comings, especially in energy density. The current commercially-available metalized PP film capacitors (based on BOPP) only offer energy density output between 1 and 2 J/cc. Based on the energy density equation, energy density $(J/cc) = \frac{1}{2} \varepsilon E^2 = \frac{1}{2} \varepsilon (V/d)^2$, a defect-free PP uniform thin film (thickness $d = 5\mu m$), dielectric constant $\varepsilon = 2.2$, and 5kV applied voltage ($E = 1000$ MV/m) can theoretically produce energy density about 10 J/cc in material level, which has been observed in our laboratory without significant increase of energy loss. To achieve Navy energy density goal (>30 J/cc), we have to either increasing PP dielectric constant to 12 or reducing the film thickness to 2.5µm. Both approaches could result in energy density ~52 J/cc, well above Navy target for electric guns (also filtering applications). Therefore, our technical approaches have been gearing toward the chemical modification of isotactic polypropylene (PP) with the structure characteristics that allow the polymer processed into the defect-free ultrathin films or exhibiting higher dielectric constant, or both. Our research approach has been two folds, including the development of (a) long chain branched PP (LCBPP) and crosslinked PP with 2-D and 3-D molecular structures, respectively, for ultrathin film preparation and (b) high dielectric PP materials, which includes the introduction of polar functional groups to prepare functional PP polymers. In addition, we have been also studying PVDF-based ferroelectric fluoropolymers that have high dielectric constants. Ideally, we could develop the material with both characteristics.

Progress:

In the first year (2005), we were focused on the development of chemistry to prepare LCBPP polymers and functional PP polymers. In LCBPP area, a new long chain branching method was developed, which involves an one-pot reaction process using Exxon-Hoechst C_2 zirconium and Mitsubishi C_1 hofnium commercial catalysts and a p-(3-butenyl)styrene "T" reagent that can simultaneously perform copolymerization and chain transfer functions. A broad range of LCBPP polymers were prepared, and the branch density is basically controlled by 3-butenylstyrene concentration in the feed. In functional PP area, we adopted our patented functionalization chemistry to prepare chain end functionalized PP polymers, which was further used to prepare PP/CuCy nano-hybrid material. The resulting single phase material (with 5% CuCy) exhibits quite high and stable dielectric constant (ε ~18) over a wide range of temperatures and frequencies (1-100 kHz), which is much higher than pure PP (ε <3). The dielectric loss maintains very low through the whole temperature and frequency ranges.

In the fiscal year (2006), we extended our LCBPP chemistry to bulk polymerization process to prepare LCBPP polymers with high molecular weight and controllable molecular structures (branch density and branch length). A series of LCBPP polymers with weight average molecular weights of between 250,000 and 500,000 g/mole and branch point densities ranging from 1 to 10 branch points per 10,000 carbons were prepared in Kg quantities. Polymer structures were characterized by ^{1}H NMR spectra and SEC with triple detection. The availability of relatively well-defined LCBPPs offered us the chance to carry out systematical examination of LCBPP properties. Special attention was focusing on the effects of LCB structure to melt rheology (oscillatory shear and extensional flow) of the LCBPPs.

In the past year (2007), our ONR research program has been focusing on dielectric properties and structure-property relationship of LCBPP polymers and PVDF-based fluoropolymers, with the objective to compare two types of dielectric materials and to find the most suitable dielectric polymer for high energy density capacitors. The desirable dielectric material should exhibit several important dielectric properties, including high breakdown voltage, low energy loss, reversible (slim) polarization-depolarization profile with a specific charge displacement vs. electric field pattern, self-heeling, etc. The detailed results are discussed below:

LCBPP Polymers
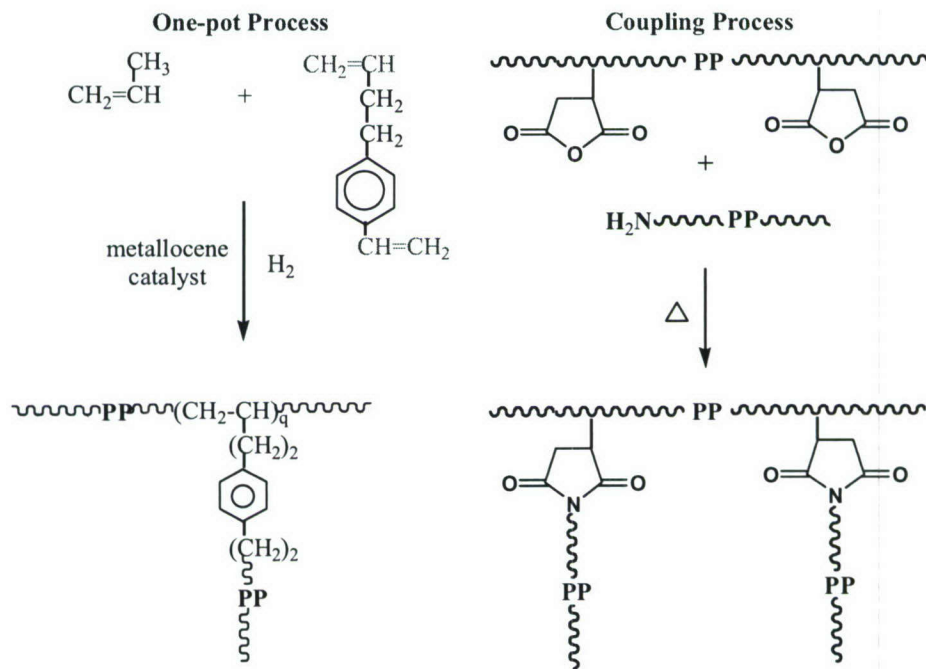
Scheme 1, Two reaction mechanisms in the preparation of LCBPP polymers.

We have developed two new synthesis routes to prepare LCBPP polymers, as illustrated in Scheme 1. The one-pot process is advantaged with a simple one-step polymerization reaction, almost the same as that of regular PP preparation. In a regular metallocene-mediated propylene polymerization, using commercial rac-Me$_2$Si[2-Me-4-Ph(Ind)]$_2$ZrCl$_2$/MAO catalyst, we introduced a branching agent, p-(3-butenyl)styrene (T-reagent) that *in situ* forms the long chain branch (LCB) structure. The catalyst maintained high activity, and the branch point density is

basically proportional to the concentration of T-reagent. On the other hand, the coupling process is advantaged with the well-defined long chain branch structure. Before forming LCB structure, both backbone and side chain PP (linear) polymers are well-characterized with known polymer molecular weight and distribution, and the branch density is basically pre-determined before mixing two. Both the required chemistries to prepare maleic anhydride modified PP backbone and amino group terminated PP side chains were developed in our group.

Table 1 compares a linear PP and several LCBPP polymers prepared by rac-Me$_2$Si[2-Me-4-Ph(Ind)]$_2$ZrCl$_2$/MAO catalyst in the presence of T-reagent, p-(3-butenyl)styrene (BSt), and a small amount of hydrogen. Catalyst activities of LCBPP1 and LCBPP2 were comparable to the homopolymerization of propylene. With higher BSt concentrations in LCBPP3 and LCBPP4, the catalyst activity was proportionally reduced, which may be associated with the slow down in chain transfer reaction to T-reagent/H$_2$. The branch point density, calculated from ^{1}H NMR spectra, was proportional to the feed concentration of BSt. It is interesting to note that on average 43% of the incorporated T-reagent was associated with branch structure, independent of BSt concentration and reaction time. LCBPP4 was run twice as long as LCBPP3 but contained similar ratios between the amounts of pendant styrene and branch points observed. These results imply that copolymerized T-reagent was immediately involved in a chain transfer reaction to form a branch point before the polymer precipitated from solution and the incorporated BSt units became inaccessible. Melting temperature, T_m, of LCBPP samples, examined by DSC, showed a gradual reduction of T_m with increase of branch density.

Table 1. Comparison of linear and LCBPP polymers prepared by *rac*-Me$_2$Si[2-Me-4-Ph(Ind)]Zr$_2$Cl$_2$/MAO mediated propylene polymerizations.

Sample	[BSt] (mol/L)	Cat. Act.[a]	M_n/$M_{w,LS}$[b] (x10^3 g/mol)	F_{BSt}[c] (mol%)	Branch Den[d]	$\eta_{0,190°C}$ (Pa·s)	Ea (kJ/mol)	M_b (g/mol)	T_m (°C)
PP	0	210	160/430	0	0.0	17,250	39	linear	158
LCBPP1	0.007	225	94/249	0.07	1.0	3,200	48	246,000	157
LCBPP2	0.013	190	91/240	0.13	1.8	3,890	49	232,000	155
LCBPP3	0.020	100	94/247	0.15	2.2	5,700	50	235,000	153
LCBPP4	0.030	64	87/256	0.21	3.3	9,030	61	238,200	153

a. catalyst activity: [kg of PP/(mmol of Zr·h)].
b. measured by SEC with light scattering detector
c. mol% of incorporated BSt
d. branch points/10,000 carbon

A broad range of LCBPP polymers have been prepared by both methods and characterized to determine their LCB molecular structures. Melt properties (essential to the thin film preparation) were examined by small amplitude dynamic oscillatory shear and elongational flow measurements. LCBPPs of similar molecular weights displayed a systematic increase in zero-shear viscosity and Arrhenius flow activation energy as branch density increased. The elongational flow was performed using an ARES rheometer equipped with the enlongational viscosity fixture. It is very interesting to see the sensitivity of LCB structure to the elongational viscosity. Figures 1 and 2 shows the extensional stress growth function, $\eta_E^+(t, \dot{\varepsilon})$ at various Hencky extension rates, $\dot{\varepsilon}$, for four well-defined LCBPP polymers that contain two and three branches with branch molecular weight 15k and 30k, respectively. At each extension rate there existed a range of deformation which perfectly tracked linear viscoelastic response. Additionally, at all extension rates studied, strain hardening was observed in all LCBPPs with a sharp increase

of $\eta_E^+(t, \dot{\varepsilon})$ above the values for the corresponding linear polymer. The value λ is defined as the ratio of maximum elongational viscosity of LCBPP vs. linear PP at $\dot{\varepsilon}$ = 0.1/sec. It is the first time to observe a clear dependence of branch length and branch density, both affecting the elongational flow.
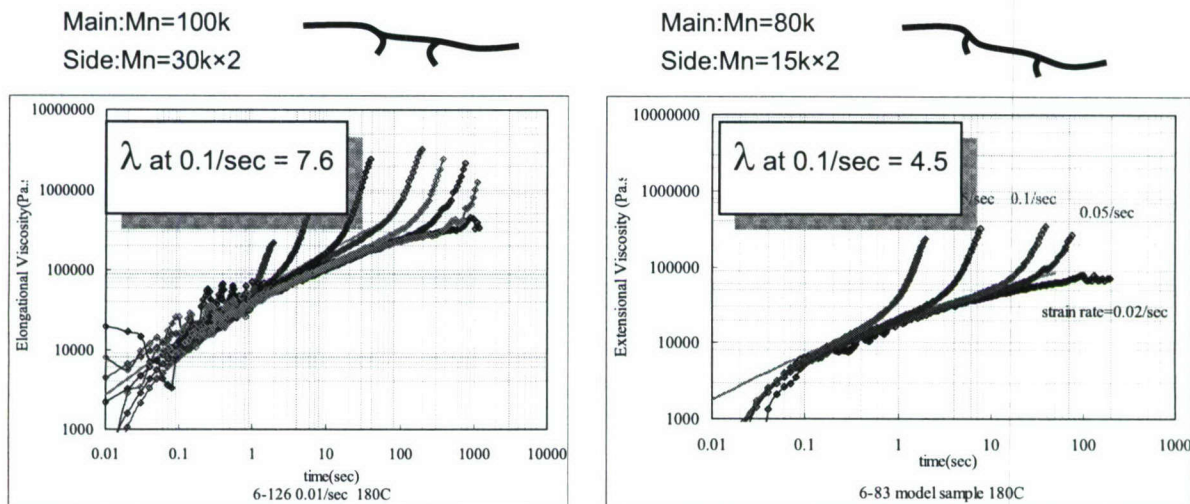

Figure 1, Extensional viscosity of two LCBPP polymers containing a similar backbone and 2 branches with 30 and 15 thousand molecular weights.
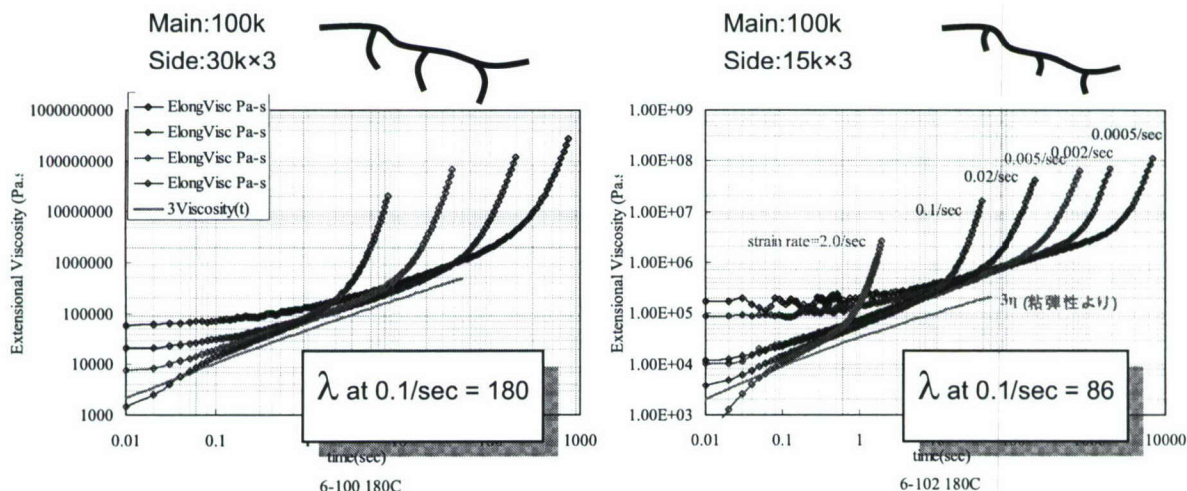

Figure 2, Extensional viscosity of two LCBPP polymers containing the same backbone and 3 branches with 30 and 15 thousand molecular weights.

Such a strain hardening is very important for processing polymer films and foams. For fabricating dielectric thin films, we collaborated with Professor Eric Baer (CWRU) and Tom Ramotowski (NUWC). Usually, the LCBPP powders were injection-molded into several test bars, then compress-molded them together into a sheet with the thickness of 200-500 μm. The resulting LCBPP sheet was bi-axially stretched at 155°C, with draw speed 400%/sec and draw ratio 8 x 8, using the bi-axial stretcher located at CWRU. Figure 3 shows a resulting bi-axially stretched PP thin film, and the stretching comparison between linear and LCB polymers. It is interesting to compare the uniformity of film thickness between LCBPP and linear PP, both have

similar molecular weight and are fabricated under the similar processing conditions. Clearly, the enlongational viscosity (strain hardening) provides LCBPP a significant edge by maintaining a uniform drawing down ratio throughout the whole bi-axially stretching process.

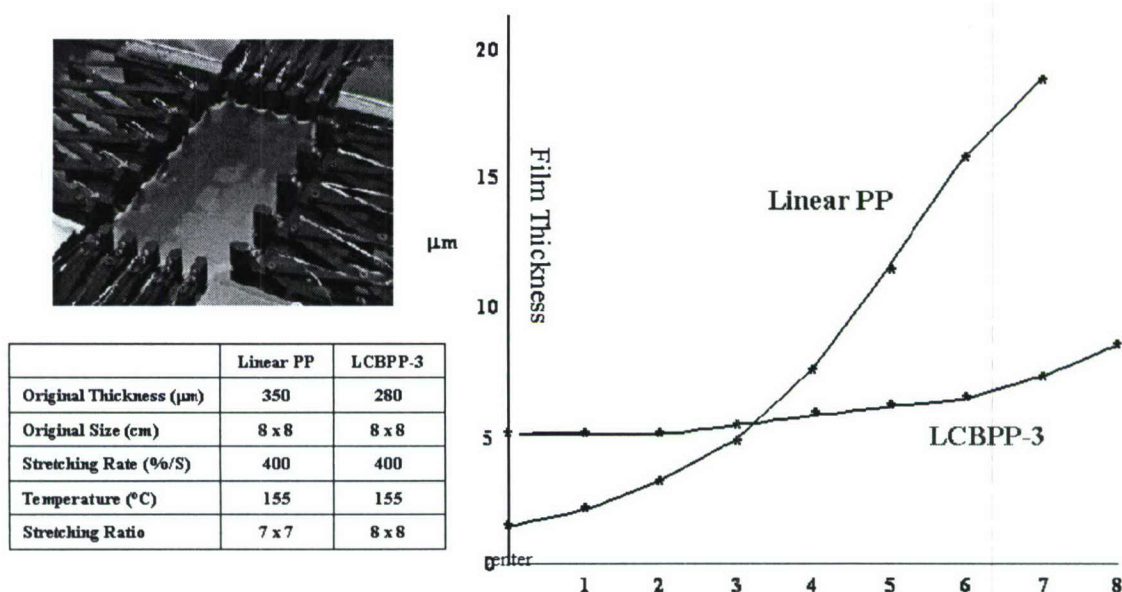|	Linear PP	LCBPP-3
Original Thickness (μm)	350	280
Original Size (cm)	8 x 8	8 x 8
Stretching Rate (%/S)	400	400
Temperature (°C)	155	155
Stretching Ratio	7 x 7	8 x 8

Figure 3. (left, top) A bi-axially stretched PP film, (left, bottom) drawing conditions for LCBPP and linear PP, and (right) film thickness of the resulting films.
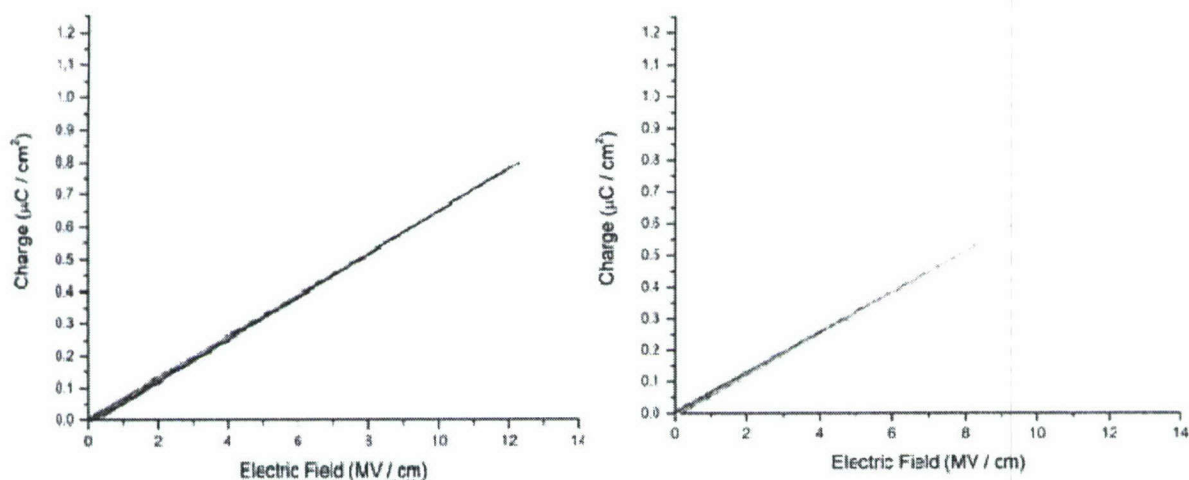

Figure 4. D-E curves of two BO-LCBPP thin film capacitors (thickness ~5 □m).

Figure 4 shows two D-E curves (charge displacement vs. unipolar electric field) of two bi-axially stretched LCBPP (BO-LCBPP) films with thickness ~5 □m. The charging-discharging cycles were first applied to 300 MV/m, then increasing 100 MV/m intervals until reaching the breakdown electric field. All BO-LCBPP polymers show extreme slim D-E curves with almost no energy loss and no remnant polarization at the end of each cycle (zero electric field). However, the breakdown strength is very difficult to predict, The D-E curve in Figure 4(left) is one of the best BO-LCBPP samples, with the breakdown electric field reaching as high as 1300

MV/m. The releasing energy density is about 13 J/cm^3, and almost no energy loss. On the other hand, the Figure 4(right) shows another BO-LCBPP sample with the result slightly better than the corresponding bi-axially stretched linear PP (BOPP) that has breakdown strength ~700 MV/m. The small difference in thin film quality (morphology, homogeneity, impurity, etc.) has a great effect to the breakdown strength.

PVDF-based Copolymers

For systematic dielectric and capacitor studies, we firstly applied a combination of the borane/O$_2$ initiation system and homogeneous solution process at ambient temperature to prepare a complete family of PVDF homo-, co-, and ter-polymers with narrow molecular weight and composition distributions and high purities. Table 2 summarizes several comparative sets of the PVDF homopolymer, VDF/TrFE and VDF/CTFE copolymers, and VDF/TrFE/CTFE terpolymers, with a systematic variation of TrFE and CTFE contents.

Table 2. Summary of VDF/TrFE/CTFE polymerization using borane/oxygen radical initiator.

Run	Reaction Conditions				Reaction Products			
	TEB/O$_2$ (mmol)	VDF/TrFE/CTFE (mL)	time (h)	Cov (%)	VDF/TrFE/CTFE (%)	Tm (°C)	Tc (°C)	∆H (J/g)
Control	--	PVDF	--	--	100/0.0/0.0	167.3	--	33.2
A-1	0.3/0.4	25.0/0.0/0.3	5	26	95.4/0.0/4.6	155.7	--	31.5
A-2	1.0/0.8	25.0/0.0/1.5	2	30	92.0/0.0/8.0	146.1	--	25.9
A-3	2.4/2.0	25.0/0.0/2.5	2	37	88.0/0.0/12.0	132.8	--	22.9
A-4	1.0/0.8	25.0/0.0/10.0	1	33	84.0/0.0/16.0	87.2	--	6.3
B-1	1.2/1.0	20.0/5.0/0.0	1.5	35	81.7/18.3/0.0	146.4	109.1	35.2
B-2	1.2/1.0	20.0/10.0/0.0	1	34	72.1/27.9/0.0	148.9	94.3	31.2
B-3	1.2/1.0	20.0/18.0/0.0	1	38	63.3/36.7/0.0	151.7	64.6	30.1
C-1	1.2/1.0	20.0/20.0/1.5	1	34	58.3/37.4/4.3	134.6	31.2	23.3
C-2	0.3/0.4	20.0/20.0/2.0	3	22	56.2/37.0/6.8	121.3	17.1	21.3
C-3	0.3/0.4	20.0/18.0/2.0	3	25	58.4/34.2/7.4	121.5	19.8	19.6
C-4	0.3/0.4	20.0/20.0/2.5	3	21	57.1/31.4/11.5	106.4	--	19.0
C-5	0.3/0.4	20.0/10.0/1.0	3	30	67/3/27.2/5.5	127.1	37.4	25.1
C-6	1.2/1.0	20.0/11.6/1.5	1	38	65.6/26.7/7.7	123.6	23.8	21.0
C-7	0.3/0.4	20.0/10.0/1.5	3	32	68.2/22.5/9.3	112.6	20.4	21.1
C-8	0.3/0.4	25.0/4.0/1.0	4	32	81.5/9.9/8.6	118.6	19.1	30.8
C-9	0.3/0.4	25.0/4.2/1.0	4	31	81.3/11.3/7.4	119.3	--	31.1
C-10	0.3/0.4	25.0/4.3/1.0	4	32	80.7/11.6/7.7	119.2	--	29.2

Both uni-polar and bi-polar polarization were examined in each sample (thin film) to obtain D-E hysteresis loops during polarization-depolarization (charging-discharging) cycles under DC and AC fields, respectively. The combination provides a detailed polarization profile with breakdown strength, energy density, energy loss, remnant polarization, coercive field, and reversibility of charge displacement under various field conditions. The non-polar PVDF and VDF/CTFE copolymers were also subjected to electric poling to form polar crystalline phase, prior to polarization-depolarization cycles.
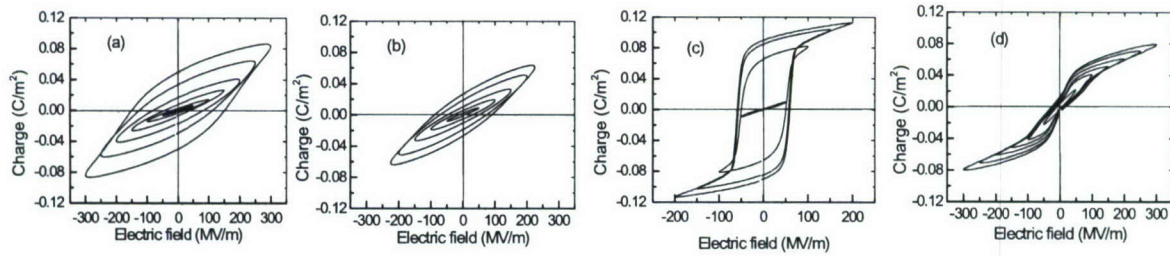
Figure 5. Bi-polar D-E hysteresis loops of (a) PVDF homopolymer (control), (b) VDF/CTFE (92.2/7.8 mol%) copolymer (run A-2), (c) VDF/TrFE (63.3/36.7 mol%) copolymer (run B-3), and (d) VDF/TrFE/CTFE (65.6/26.7/7.7 mol %) terpolymer (run C-6).

Figure 5 compares bi-polar D-E hysteresis loops of four representative semi-crystalline fluoropolymers, including the PVDF homopolymer (control), VDF/CTFE (92.2/7.8 mol%) copolymer (run A-2), VDF/TrFE (63.3/36.7 mol%) copolymer (run B-3), and VDF/TrFE/CTFE (65.6/26.7/7.7 mol%) terpolymer (run C-6), which exhibit four polarization profiles. A sinusoidal AC electric field (50 Hz) was applied across the polymer film with an initial amplitude of 50 MV/m, then increasing 50 MV/m intervals until reaching 300 MV/m. In comparing Figures 5 (a) and 5 (b), both the PVDF and VDF/CTFE (92.2/7.8 mol%) copolymer show similar (oval-shape) D-E hysteresis loops, even up to 300 MV/m. In general, the charge displacement increases following the applied electric field. The hysterisis loop accompanied with remnant polarization (E = 0) and a coercive field (P= 0), both gradually enlarge with the increasing field amplitude. Since there is a presence of remnant polarization, the coercive field is required in order to neutralize the remnant dipoles while the field is switched to the opposite direction, which results in a large D-E hysteresis loop (i.e. large remnant polarization and coercive field) and energy loss (>70% in high fields). Both PVDF and VDF/CTFE copolymers are not suitable for AC capacitor applications. Figure 5 (c) shows a large (square-shape) D-E hysterisis loop for the VDF/TrFE (63.3/36.7 mol %) copolymer, with a large coercive field (E_{coe} ~50 MV/m) and remnant polarization (P_{rem}= 0.08 C/m^2) that is only slightly smaller than the maximum polarization (P_{max}= 0.11 C/m^2) in the D-E loop at E= 200 MV/m. Overall, the results indicate a strong irreversibility of the oriented polar β-phase crystal that maintains its orientation along the field direction even after complete removal of the applied electric field. The inevitable huge energy loss (>90%) in all fields >100 MV/m prevents any consideration for using ferroelectric VDF/TrFE copolymers in AC capacitor applications. On the other hand, the corresponding VDF/TrFE/CTFE (65.6/26.7/7.7 mol%) terpolymer (Figure 5 (d)) has a similar VDF content but contains few bulky Cl atoms along the polymer chain, which reduce the crystalline size and change chain conformation to a *TTTGTTTG'* conformation (γ-phase crystal). The terpolymer exhibits common relaxed ferroelectric behaviors with a Curie temperature (maximum dielectric constant) at near ambient temperature. In other words, it is only required a little bit of activation energy in phase transition. Consequently, the terpolymer shows a slim D-E hysteresis loop at ambient temperature, with very small remnant polarization (P_{rem}< 0.01 C/m^2 at E= 0) and coercive field (E_{coe}< 10 MV/m at P= 0) even after applying E= 300 MV/m. Overall, the polar γ-phase crystals are easily aligned with the applied electric field to a high polarization level (P_{max}= 0.078 C/m^2 at E= 200 MV/m), and they are also easily disoriented after removing the applied electric field. This highly reversible polarization in both directions is an essential feature in the AC high energy density capacitors with high energy density and low energy loss.
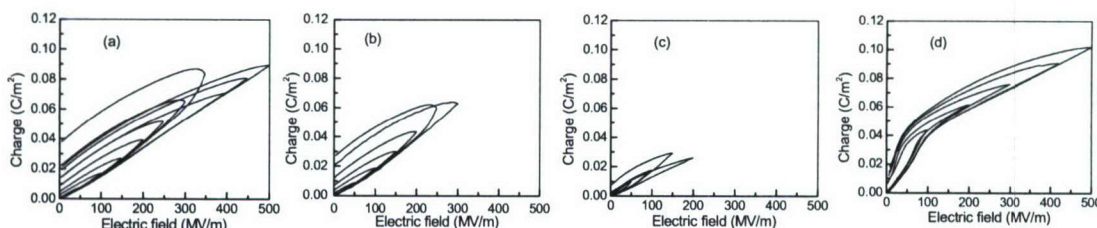
Figure 6. Uni-polar D-E hysteresis loops of (a) PVDF homopolymer (control), (b) VDF/CTFE (92.2/7.8 mol%) copolymer (run A-2), (c) VDF/TrFE (63.3/36.7 mol%) copolymer (run B-3), and (d) VDF/TrFE/CTFE (65.6/26.7/7.7 mol %) terpolymer (run C-6).

Figure 6 compares uni-polar D-E hysteresis loops of the same set of the PVDF homopolymer (control), VDF/CTFE (92.2/7.8 mol %) (run A-2) and VDF/TrFE (63.3/36.7 mol %) (run B-3) copolymers, and the VDF/TrFE/CTFE (65.6/26.7/7.7 mol %) terpolymer (run C-6). Since uni-polar measurement does not require the dipole to flip into the opposite direction, the remnant polarization at zero field becomes a permanent (saturated) dipole and is not involved in the subsequent polarization-depolarization (charging-discharging) cycles. Therefore, there is no coercive field observed in all uni-polar D-E curves. The contrast is most obvious in the VDF/TrFE (63.3/36.7 mol%) copolymer (run B-3), with a thin and small uni-polar D-E loop in Figure 6 (c) vs. wide and large bi-polar D-E loops in Figure 5 (c). Only a small portion of CF_2 dipoles in the VDF/TrFE copolymer responds to the uni-polar electric field. In DC fields, most of the dipoles are simply freezed and become remnant polarization after the first polarization-depolarization cycle. In addition, the breakdown voltage is also relatively low at about 200 MV/m. This inherent irreversibility of polarization makes the ferroelectric VDF/TrFE copolymers almost impossible for any capacitor applications. In Figure 6 (a), there is a clear poling-induced phase transition at the electric field of about 300 MV/m, with a simultaneous jump in the polarization level and dielectric loss. The subsequent hysteresis loops at higher electric fields return to the normal (thinner) shape and level. The results imply that most of the formed polar domains only contribute to the remnant polarization and have a limited effect on the D-E loops under DC fields. Most of the dielectric loss in these unipolar D-E loops may be due to the conduction mechanisms associated with the amorphous phase, which will be discussed later. A similar result was observed in Figure 6 (b) for the VDF/CTFE (92.2/7.8 mol %) copolymer that shows a smaller phase transition at a lower electric field (250 MV/m).

It seems that the most desirable polymer is the polar polymer with a combination of high crystallinity and small crystal size, similar to those in relaxed ferroelectric materials. Figure 6 (d) shows the uni-polar D-E loops for the VDF/TrFE/CTFE (65.6/26.7/7.7 mol%) terpolymer (run C-6) with relaxed ferroelectric properties, exhibiting a high dielectric constant and Curie temperature at near ambient temperature. The slim uni-polar D-E loops are almost overlapped within the upper half of the corresponding bi-polar D-E curves in Figure 5 (d). As discussed before, most of the polar γ-phase crystals aligned with the electric field were disoriented after the removal of the applied electric field. There is almost no remnant polarization. In addition, the terpolymer shows a high breakdown electric field ~500 MV/m. The electric displacement reached 0.1 C/m^2 at E= 500 MV/m, which reaches the theoretical value of 0.13 C/m^2 for the fully polarized (β-phase) PVDF homopolymer. This terpolymer almost reached its limit with almost all CF_2 groups in VDF and TrFE units reversibly polarized along the electric field.

The desirable features in VDF/TrFE/CTFE terpolymers prompted us to systematically examine the whole series of terpolymer compositions in order to understand the structure-property relationship and to identify the most suitable material for DC capacitor applications. Figures 7 and 8 compares the total energy charged, energy released (energy density), and energy loss of the two sets of terpolymers. One set having a fixed CTFE content and a varying VDF/TrFE mole ratio, and the other set having a fixed VDF content and a varying TrFE/CTFE mole ratio. Figure 9 shows their energy storage efficiency by dividing the total releasing energy (energy density) over the total energy charged in each cycle with various DC electric fields.
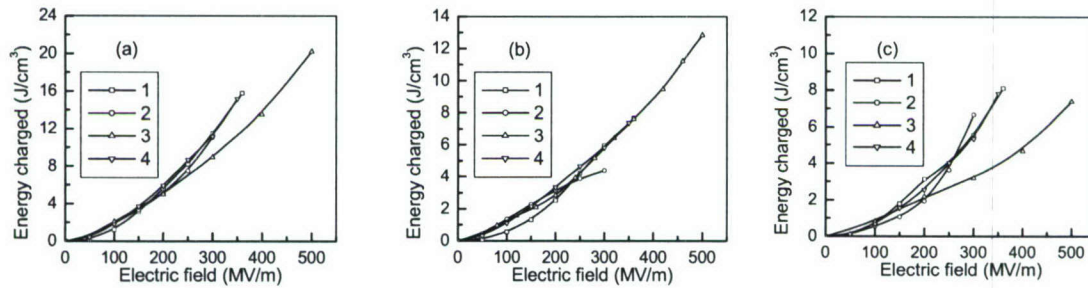

Figure 7. Comparison of (a) total energy charged during the charging cycle, (b) energy released during the discharge cycle (energy density), and (c) energy loss for the first set of the VDF/TrFE/CTFE terpolymers with (1) 92.2/0/7.8 (run A-2), (2) 80.7/11.6/7.7 (run C-10), (3) 65.6/26.7/7.7 (run C-6), and (4) 58.4/34.2/7.4 mol% (run C-3).
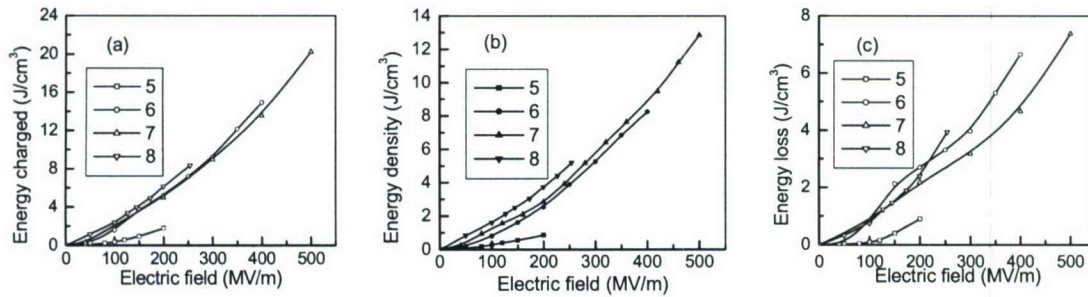

Figure 8. Comparison of (a) total energy charged during the charging cycle, (b) energy released during the discharge cycle (energy density), and (c) energy loss for the second set of the VDF/TrFE/CTFE terpolymers with (5) 63.3/36.7/0 (run B-3), (6) 67.327.2/5.5 (run C-5), (7) 65.626.7/7.7 (run C-6), and (8) 68.2/22.5/9.3 mol% (run C-7).

In Figure 7, comparing with the spontaneously poled VDF/TrFE/CTFE (65.6/26.7/7.7) terpolymer (run C-6), both the poled VDF/CTFE (92.2/7.8 mole%) copolymer (run A-2) and VDF/TrFE/CTFE (80.7/11.6/7.7 mol%) terpolymer (run C-10) show higher energy charged (Figure 7 (a)), but almost the same energy discharged (Figure 7 (b)), at above 200 MV/m. In other words, a significant higher energy loss (Figure 7 (c)) is observed in the poled samples, and the energy storage efficiency is < 50% at the applied DC electric field > 300 MV/m (Figure 9 (a)). On the other hand, the spontaneously poled VDF/TrFE/CTFE (65.6/26.7/7.7) sample shows a smooth increase of energy charged and energy released (about 13 J/cm^3 at 500 MV/m), and a stable energy storage efficiency (> 60%) throughout a wide range of electric fields. However, the VDF/TrFE/CTFE (58.4/34.2/7.4) terpolymer (run C-3), with Curie temperature (19.8 °C) below

ambient temperature, shows an early dielectric saturation at about 200 MV/m and the maximum energy density of only about 4 J/cm^3. The energy loss also shapely increases above 200 MV/m, indicating that most of the energy charged is lost after 200 MV/m. The overall energy storage efficiency at breakdown (E= 300 MV/m) is only about 40% (Figure 9 (a)). The paraelectric phases of this terpolymer may fail to engage in the polarization-depolarization cycle.
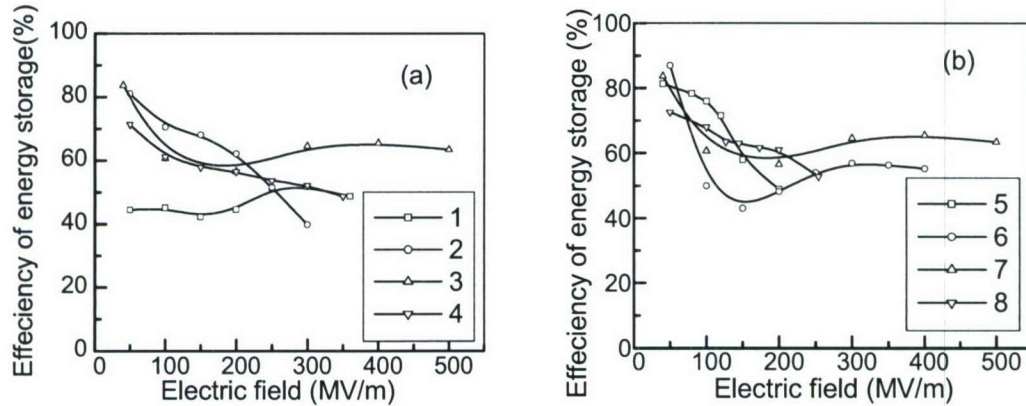

Figure 9. Comparison of energy storage efficiency of (a) the first set of VDF/TrFE/CTFE terpolymers containing (1) 92.2/0/7.8 (run A-2), (2) 80.7/11.6/7.7 (run C-10), (3) 65.6/26.7/7.7 (run C-6), and (4) 58.4/34.2/7.4 mol% (run C-3), (b) the second set of the VDF/TrFE/CTFE terpolymers containing (5) 63.3/36.7/0 (run B-3), (6) 67.327.2/5.5 (run C-5), (7) 65.626.7/7.7 (run C-6), and (8) 68.2/22.5/9.3 mol% (run C-7).

In Figure 8, all three terpolymers are spontaneously formed γ-phase crystals with the crystal size and degree of crystallinity inversely proportional to the CTFE content. The charged and discharged energy during the polarization-depolarization cycle follows the general trend. But, the VDF/TrFE/CTFE (65.6/26.7/7.7 mol%) terpolymer (run C-6) with Curie temperature at near ambient temperature seems most desirable with the highest breakdown strength, energy density, and energy storage efficiency. Both VDF/TrFE/CTFE terpolymers with slightly higher CTFE content (68.2/22.5/9.3 mol%, run C-7)—resulting in increase of amorphous phase—and slightly low CTFE content (67.3/27.2/5.5 mol%, run C-5)—resulting in a larger crystal size—show significantly low breakdown strength and high energy loss. Figure 9 (b) clearly shows VDF/TrFE/CTFE (65.6/26.7/7.7 mol%) terpolymer (run C-6) possessing highest energy storage efficiency and breakdown electric field. As discussed, the key balance act in the terpolymer composition is to tune its Curie temperature toward ambient temperature, with small γ-crystal size and high crystallinity.

This study systematically examines the structure-property relationship of PVDF-based polymers, containing TrFE units (controlling chain conformation) and CTFE units (tuning crystal structure), with the objective to understand their polarization-depolarization profiles under both DC and AC fields. The most desirable fluoropolymer structure has a polar crystalline structure with high crystallinity and small crystal domains (i.e. *TTTG* chain conformation and γ-phase crystal). The polymer exhibit a relaxed ferroelectric behavior with a slim D-E hysterysis loop and a high dielectric constant at the operation temperature (ambient temperature in this case). The relaxed ferroelectric VDF/TrFE/CTFE (65.6/26.7/7.7 mol%) terpolymer (run C-6) with the

desirable structure shows a good combination of dielectric properties with a high dielectric constant (ε >60) at Curie temperature (~25 °C), high breakdown voltage (~500 MV/m), high energy density ~13 J/cm^3 with the energy storage efficiency ~60%. Comparing with the current state-of-the-art capacitor technology, the high dielectric fluoropolymer significantly increases the energy density, but generates more energy loss (~40%). Both LCBPP and fluoropolymer systems are far from the ideal dielectric material for achieving high energy density and high storage efficiency (Figure 10).
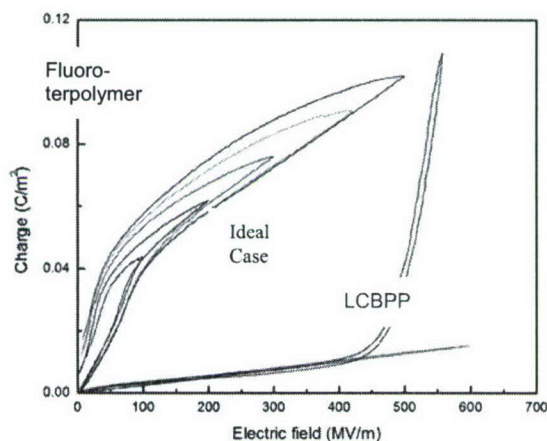

Figure 10, Comparison of D-E curves for LCBPP, VDF/TrFE/CTFE (65.6/26.7/7.7) fluoropolymer, and an ideal pattern for high density capacitor.

Papers and Patent Resulting From This Award

Papers

1. A New Synthetic Route to Borane-Terminated Isotactic Polypropylenes via Styrene/Hydrogen Consecutive Chain Transfer Reaction, G. Fan, J. Y. Dong, Z. Wang, and T. C. Chung, J. Polym. Sci., Polym. Chem. Ed. 44, 539-548, **2005**.

2. Metallocene Catalysts for Olefin Polymerization, T. C. Chung, *Encyclopedia of Chemical Processing*, Edited by S. Lee, Marcel Dekker, 1599-1614, **2006**.

1. Nano-sized Rubber Balls Toughen Plastics and Enhance Their Environmental Stability, T. C. Chung, *MRS Bulletin* **2006**, 31, 185.

2. Reaction Mechanism of Borane/Oxygen Radical Initiators During the Polymerization of Fluoromonomers, Zhi-cheng Zhang and T. C. Mike Chung, *Macromolecules* **2006**, 39, 5187.

3. High Dielectric VDF/TrFE/CTFE Terpolymers Prepared by Hydrogenation of VDF/CTFE Copolymers; Synthesis and Characterization, Zhiming Wang, Zhicheng Zhang, and T. C. Mike Chung, *Macromolecules* **2006**, 39, 4268.

4. New 1-Decene Based LLDPE Resins and Comparison with the Corresponding 1-Octene and 1-Hexene Based LLLDPE Resins, H, Hong, Z. C. Zhang, T. C. Chung, and R. W. Lee, *J. Polym. Sci., Polym. Chem. Ed.* **2007**, 45, 639.

5. Synthesis and Characterization of Long Chain Branched Isotactic Polypropylene (LCBPP) via Metallocene Catalyst and T-reagent, Justin A. Langston and T. C. Mike Chung, *Macromolecules* **2007**, 40, 2712.

6. Fluoro-terpolymer Based Capacitors Having High Energy Density, Low Energy Loss, and High Pulsed Charge-discharge Cycles, Zhicheng Zhang, and T. C. Mike Chung, *Macromolecules* **2007**, 40, 783.

7. Synthesis and Characterization of Long Chain Branched Isotectic Polypropylene via Metallocene Catalyst and T-Reagent, J. A. Langston and T. C. Mike Chung, *SPE* (2007).

8. Synthesis of Chain End Functional Fluoropolymers by Functional Borane Initiators and Application in The exfloriated Fluoropolymer/Clay Nanocomposites, ZhiCheng Zhang, Zhiming Wang, and T. C. Mike Chung, *Macromolecules* **2007**, 40, 5235.

9. One-pot Synthesis of Long Chain Branched PP (LCBPP) Using Ziegler-Natta Catalyst and Branching Reagents, Justin A. Langston, Ralph H. Colby, Fumihiko Shimizu, Toru Suzuki, Masaru Aoki, and T. C. Mike Chung, *Macromolecular Symposia* **2007**, 260, 34.

10. The Structure-Property Relationship of PVDF-based Polymers with Energy Storage and Loss under Applied Electric Fields Zhicheng Zhang, T. C. Mike Chung, *Macromolecules* **2007**, 40, 9391.

11. Borane-mediated Control Radical Polymerization; Synthesis of Chain End Functonalized Fluoropolymers, T. C. Chung, H. Hong, Z. C. Zhang, and Z. M. Wang, ACS Symposium Series. No. 944, Pages 387-403 "Controlled/Living Radical Polymerization" Edited by K. Matyjaszewski.

12. Control of Molecular Weight and Chain End Group in Tactic Polypropylene Using Chain Transfer Agents, T. C. Chung, CRC Book "Catalysis for Stereoregulating Polymerization", Ed. By L. Baugh, J. A. Canich, and B. Coughlin.

13. Functionalization and Chemical Modification of Syndiotactic Polystyrene, T. C. Mike Chung, John Wiley & Sons Book *"Syndiotactic Polystyrene: Synthesis, Characterization, Processing, and Applications"* Edited by Jurgen Schellenberg.

Patents

1. Exfoliated Polyolefin/Clay Nano-composites Using Chain End Functionalized Polyolefin As the Polymeric Surfactant, T. C. Chung, E. Manias, and Z. M. Wang, *International Patent Number WO2005044904* and *European Patent Application No./Patent No.* 04816777.9-2102-US2004023179 (**2006**).

2. Functional Fluoropolymers and Process Therefore, T. C. Chung, H. Hong, M. Oka, and K. Kubo, *International Patent Number WO* 2005085298 A1 and *European Patent Application No./Patent No.* 04711840.1-2109-US2004004578 (**2006**).

3. Telechelic Polymers Containing Reactive Functional Groups, T. C. Chung, H. Hong, M. Oka, and K. Kubo, *International Patent Number WO* 2005085297 A1 and *European Patent Application No//Patent No.* 04711824.5-2109-US2004004584 (**2006**).

4. One-pot Process of Reagents for Preparing Long Chain Branched Polymers, T. C. Chung, *International Publication Number WO* 2006/007512 A1 and *European Patent Application/Patent No.* 05763536.9-1220-US2005023151 (**2007**).

5. Process of Preparing Functional Fluoropolymers, T. C. Chung, H. Hong, M. Oka, and K. Kubo, *U. S. Patent* 7,220,807 (**2007**).

6. Exfoliated Polyolefin/Clay Nano-composites Using Chain End Functionalized Polyolefin As the Polymeric Surfactant, T. C. Chung, E. Manias, and Z. M. Wang, *U. S. Patent* 7,241,829 (**2007**).

7. One-pot Process of Preparing A Long Chain Branched Polyolefin Using A Dual Function T Reagent, T. C. Chung, U. S. Patent Application No. 11/170,698.

8. Chain End Functionalized Fluoropolymers Having High Dielectric Constant and Good Chemical Reactivity, Z. C. Zhang, S. T. Chen, T. C. Mike Chung, K. Kubo, and K. Kigawa, U. S. Patent Application No. 11/541,781.